

DRAW: Defending Camera-shot RAW against Image Manipulation

Xiaoxiao Hu^{1,2*}, Qichao Ying^{1,2*}, Zhenxing Qian^{1,2†}, Sheng Li^{1,2}, Xinpeng Zhang^{1,2}

¹School of Computer Science, Fudan University

²Key Laboratory of Culture & Tourism Intelligent Computing, Fudan University

Abstract

RAW files are the initial measurement of scene radiance widely used in most cameras, and the ubiquitously-used RGB images are converted from RAW data through Image Signal Processing (ISP) pipelines. Nowadays, digital images are risky of being nefariously manipulated. Inspired by the fact that innate immunity is the first line of body defense, we propose DRAW, a novel scheme of defending images against manipulation by protecting their sources, i.e., camera-shot RAWs. Specifically, we design a lightweight Multi-frequency Partial Fusion Network (MPF-Net) friendly to devices with limited computing resources by frequency learning and partial feature fusion. It introduces invisible watermarks as protective signal into the RAW data. The protection capability can not only be transferred into the rendered RGB images regardless of the applied ISP pipeline, but also is resilient to post-processing operations such as blurring or compression. Once the image is manipulated, we can accurately identify the forged areas with a localization network. Extensive experiments on several famous RAW datasets, e.g., RAISE, FiveK and SIDD, indicate the effectiveness of our method. We hope that this technique can be used in future cameras as an option for image protection, which could effectively restrict image manipulation at the source.

1. Introduction

In the digital world, the credibility of the famous saying “seeing is believing” is largely at risk since nowadays people can easily manipulate critical content within an image and redistribute the fabricated version via the Internet. Owing to the fact that readers are more susceptible to well-crafted misleading material, fabricated images can be a means for some politicians to sway public opinion. In more severe cases, those fraudulent images can be used to bolster fake news or criminal investigation.

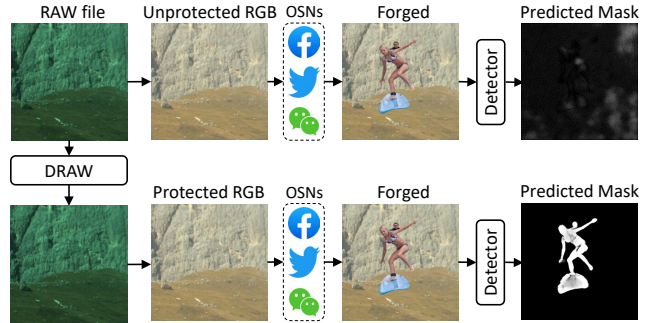


Figure 1. DRAW improves the performance of image manipulation localization against lossy image operations via imperceptible protective signal injection into RAW files.

Image manipulation detection [11, 55] and localization [12, 75] has become a critical area of research for decades, with the goal of distinguishing manipulated images from authentic ones and locating the manipulated areas. While early methods mainly check the integrity of the images from statistical aspects, e.g., the Photo-Response Non-Uniformity (PRNU) noise [11] and the fixed pattern noise (FPN) [39], the uprising of deep networks has greatly strengthened the capability to find traces left by a variety of manipulation [12, 77, 32]. However, the adversary is also continuously evolving both in strength and diversity. For example, recent deep-network-based image editing algorithms [67, 19] are reported to produce highly realistic images with almost no visible artifacts near the edges. Therefore, it remains a big issue whether the learned subtle forensics traces can always be present in the newly forged images. Also, though some works [75, 76] explicitly handle lossy online transmission scenarios, they still face limited performance against well-crafted forgeries, e.g., inpainting, or lossy image operations, e.g., Gaussian blurring.

Inspired by the fact that innate immunity is the first line of body defense and the best weapon to mitigate diseases, safeguarding images against manipulations is an alternative and promising way of deterring malicious attackers. Indeed, the ubiquitous 8-bit RGB images are not the pristine format for reflecting how we perceive the world. They are converted from RAW files via ISP pipelines. Therefore, we

*Xiaoxiao Hu and Qichao Ying contribute equally to this work.

†Corresponding author: Zhenxing Qian (zxqian@fudan.edu.cn)

propose DRAW, a proactive image protection scheme that defends camera-shooted RAW data against malicious manipulation on the RGB domain. Specifically, we propose to introduce imperceptible protective signal into the RAW data, which can be transferred into the rendered RGB images, even though various types of ISP pipelines are applied. Once these images are manipulated, the localization networks can exactly localize the forged areas regardless of image post-processing operations such as blurring, compression or color jittering. Besides, a novel Multi-frequency Partial Fusion Network (MPF-Net) is proposed to implement RAW protection, which adopts frequency learning and cross-frequency partial feature fusion to significantly decrease the computational complexity. We illustrate the functionality of DRAW in Fig. 1, which promotes accurate manipulation localization without affecting the visual quality.

Extensive experiments on several famous RAW datasets, e.g., RAISE, FiveK and SIDD, prove the imperceptibility, robustness and generalizability of our method. Besides, to compare RAW-domain protection with previous works, we tempt to borrow the success of RGB-domain protection [4, 96, 83] as the baseline method for proactive manipulation localization. The results show that DRAW hosts a noticeable performance gain and a nontrivial benefit of content-related adaptive embedding. In addition, MPF-Net provides superior performance compared to classical U-Net [58] architecture with only 20.9% of its memory cost and 0.95% of its parameters. The novel lightweight architecture makes it possible to be integrated into cameras in the future, thereby changing the current situation where digital images can be freely manipulated.

The contributions of this paper are three-folded, namely:

1. DRAW is the first to propose RAW protection against image manipulation. The corresponding RGB images will carry imperceptible protective signal even though various types of imaging pipelines or lossy image operations are applied.
2. With RAW protection, image manipulation localization networks can better resist lossy image operations such as JPEG compression, blurring and rescaling.
3. A novel lightweight MPF-Net is proposed for integrating RAW protection into cameras in the future, thereby potentially changing the current situation where digital images can be freely manipulated.

2. Related Works

Passive Image Manipulation Localization. Many existing image forensics schemes are designed to detect special kinds of attacks, e.g., splicing detection [75, 59], copy-moving detection [33, 45] and inpainting detection [99, 42]. In addition, some universal tampering detection

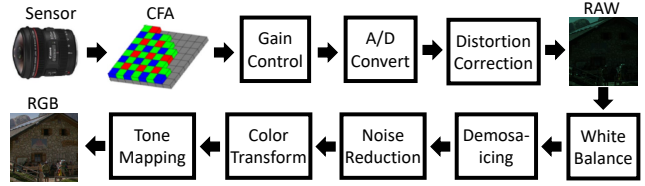


Figure 2. Typical camera imaging pipeline for RAW data acquisition and subsequent RGB image signal processing.

schemes [12, 77, 32] exploit universal noise artifacts left by manipulation. Mantra-Net [77] uses fully convolutional networks, Z-Pooling and long short-term memory cells for pixel-wise anomaly detection. MVSS-Net [12] jointly exploits the noise view and the boundary artifact using multi-view feature learning and multi-scale supervision. RGB-N [97] additionally utilizes auto-generated data augmentation for training. RIML [75] includes adversarial training, where the lossy Online Social Network (OSN) transmission is simulated by modeling noise from different sources. However, these works are still limited in generalization to well-crafted manipulations or heavy lossy operations.

Watermarking for Image Protection. Many image protection schemes based on watermarking [51, 35, 24, 82] have been proposed. Asnani et al. [4] propose to embed templates into images for more accurate manipulation detection. Zhao et al. [96] embed watermarks as anti-Deepfake labels into the facial identity features. FakeTagger [71] embeds the identity information into the whole facial image, which can be recovered after illegal face swapping. Khachaturov et al. [37] and Yin et al [81] respectively propose to attack inpainting or Super-Resolution (SR) models by forcing them to work abnormally on the targeted images. However, these approaches do not tackle the issue of forgery localization, and many of them cannot combat lossy image operations. We alternatively introduce imperceptible protective signal into RAW data and transfer it into RGB images to aid robust manipulation localization.

Models for Limited Computing Resources. Classical network architectures for segmentation-based tasks, e.g., U-Net [58] or FPN [47], usually require non-affordable computing resources for many small devices. MobileNet [30] and ShuffleNet [52] are early works on addressing this issue respectively via Depth-wise Separable Convolution (DSConv) and channel split & shuffle. ENet [54] proposes an asymmetric encoder-decoder architecture with early downsampling. SegNet [6] only stores the max-pooling indices of the feature maps and uses them in its decoder network to achieve good performance. Despite substantial efforts made, these networks are either still computationally demanding or sacrifice performance for model size shrinkage. We propose MPF-Net that contains only 20.9% of memory cost and 0.95% of parameters of U-Net yet provides surpassing performance in our task.

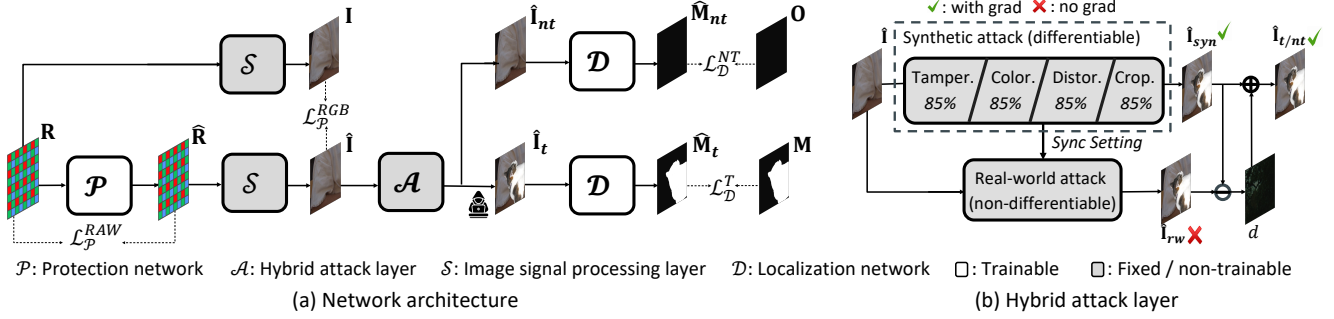


Figure 3. **Pipeline design of DRAW.** We design a lightweight protection network that embeds imperceptible protective signal in the RAW domain and transfers it into the rendered RGB images. On the recipient’s side, the localization network identifies the forged areas.

3. Proposed Method

3.1. Approach

Fig. 3 depicts the pipeline design of DRAW. We denote the captured RAW data as \mathbf{R} , and use a protection network \mathcal{P} to transform \mathbf{R} into the protected RAW, i.e., $\hat{\mathbf{R}}$. The functionality of \mathcal{P} is to adaptively embed a transferrable protective signal into $\hat{\mathbf{R}}$ for robust and accurate image manipulation localization in the RGB domain. Considering the computational limitation of imaging equipment, we use a novel lightweight MPF-Net specified in Section 3.2 to implement \mathcal{P} . Next, we use the ISP layer \mathcal{S} to render $\hat{\mathbf{R}}$ into the protected RGB image $\hat{\mathbf{I}}$. Provided with a number of off-the-shelf deep-network-based ISP algorithms and non-differentiable conventional ISP algorithms, during training, we include a popular conventional method, i.e., LibRaw [1] and two deep-learning methods, i.e., CycleISP [87] and In-vISP [78], and leave other ISP algorithms [86, 2] for evaluation. To improve generalizability, interpolation is conducted on one network-rendered RGB $\hat{\mathbf{I}}_{net}$ and one conventional-algorithm-generated RGB $\hat{\mathbf{I}}_{conv}$ to produce $\hat{\mathbf{I}}$, i.e., $\hat{\mathbf{I}} = \omega \cdot \hat{\mathbf{I}}_{conv} + (1 - \omega) \cdot \hat{\mathbf{I}}_{net}$, where ω is uniformly within $[0, 1]$.

Afterward, to simulate image redistribution of $\hat{\mathbf{I}}$, we include the hybrid attack layer \mathcal{A} to perform manipulation and lossy operations on $\hat{\mathbf{I}}$. It comprises of modules for tampering, color adjustments, distortions (lossy operations) and cropping. In line with typical forgery detection works [12, 75], we consider inpainting, splicing and copy-moving as the most common three types of tampering, which often alter the underlying meaning of an image. In contrast, color adjustment and distortion are often considered benign yet can potentially erase traces for manipulation localization. During training, these modules can be conditionally performed according to the empirical *activation possibilities* (85%) and in any arbitrary ordering to encourage diversity, e.g., tampering then distorting, cropping then tampering, etc. We respectively denote the attacked images as $\hat{\mathbf{I}}_t$ if the tampering module is activated or $\hat{\mathbf{I}}_{nt}$ if otherwise. The latter is identified as authentic images,

whose introduction is to explicitly minimize the false alarm rate of DRAW. Detailed implementations of the modules are specified in the supplement. Besides, to closer the gap between real and simulated lossy operations and color jittering operations, we add the difference between $\hat{\mathbf{I}}_{syn}$ and $\hat{\mathbf{I}}_{rw}$ on to $\hat{\mathbf{I}}_{syn}$, where $\hat{\mathbf{I}}_{syn}$ and $\hat{\mathbf{I}}_{rw}$ respectively denote synthetic and real-world processed image using the same setting. $x = \hat{\mathbf{I}}_{syn} + sg(\hat{\mathbf{I}}_{rw} - \hat{\mathbf{I}}_{syn})$, $x \in \{\hat{\mathbf{I}}_t, \hat{\mathbf{I}}_{nt}\}$, where sg stands for the stop-gradient operator [7].

On the recipient’s side, we use the localization network \mathcal{D} to estimate the manipulated region given a doubted image that could be one of $\hat{\mathbf{I}}_t$ or $\hat{\mathbf{I}}_{nt}$. If it’s an manipulated image $\hat{\mathbf{I}}_t$, the predicted mask $\hat{\mathbf{M}}_t$ should be close to the ground-truth \mathbf{M} . Otherwise, it should be close to a zero matrix. DRAW is flexible on the selection of \mathcal{D} , where many off-the-shelf networks can be applied, e.g., DRAW-HRNet [65], DRAW-MVSS [12] or DRAW-RIML [75].

Objective Loss Functions. We need to include fidelity terms \mathcal{L}_P^{RAW} and \mathcal{L}_P^{RGB} to ensure imperceptible protection. We find that the ℓ_1 distance is the best in practice to minimize modification compared to many advanced deep-network-based terms, e.g., Lpips loss [89] and contextual loss [91].

$$\begin{aligned} \mathcal{L}_P^{RAW} &= \mathbb{E}_{\mathbf{R}} [\|\mathbf{R} - \mathcal{P}(\mathbf{R})\|_1], \\ \mathcal{L}_P^{RGB} &= \mathbb{E}_{\mathbf{R}} [\|\mathcal{S}(\mathbf{R}) - \mathcal{S}(\mathcal{P}(\mathbf{R}))\|_1]. \end{aligned} \quad (1)$$

Next, we include localization terms to minimize the Binary Cross Entropy (BCE) losses that respectively compare $\hat{\mathbf{M}}_t$ with \mathbf{M} , and $\hat{\mathbf{M}}_{nt}$ with a zero matrix.

$$\begin{aligned} \mathcal{L}_D^T &= -\mathbb{E}_{\hat{\mathbf{I}}_t} \left[\mathbf{M} \log \left(\mathcal{D}(\hat{\mathbf{I}}_t) \right) + (1 - \mathbf{M}) \log \left(1 - \mathcal{D}(\hat{\mathbf{I}}_t) \right) \right], \\ \mathcal{L}_D^{NT} &= -\mathbb{E}_{\hat{\mathbf{I}}_{nt}} \left[\log \left(1 - \mathcal{D}(\hat{\mathbf{I}}_{nt}) \right) \right]. \end{aligned} \quad (2)$$

The total loss for DRAW is shown in Eq. (3), where $\alpha, \beta, \gamma, \epsilon$ are empirically-set hyper-parameters.

$$\begin{aligned} \mathcal{L} &= \alpha \cdot \mathcal{L}_P^{RAW} + \beta \cdot \mathcal{L}_P^{RGB} + \gamma \cdot \mathcal{L}_D^T + \epsilon \cdot \mathcal{L}_D^{NT}, \\ \alpha &= 10, \beta = 1, \gamma = 0.02, \epsilon = 0.01. \end{aligned} \quad (3)$$

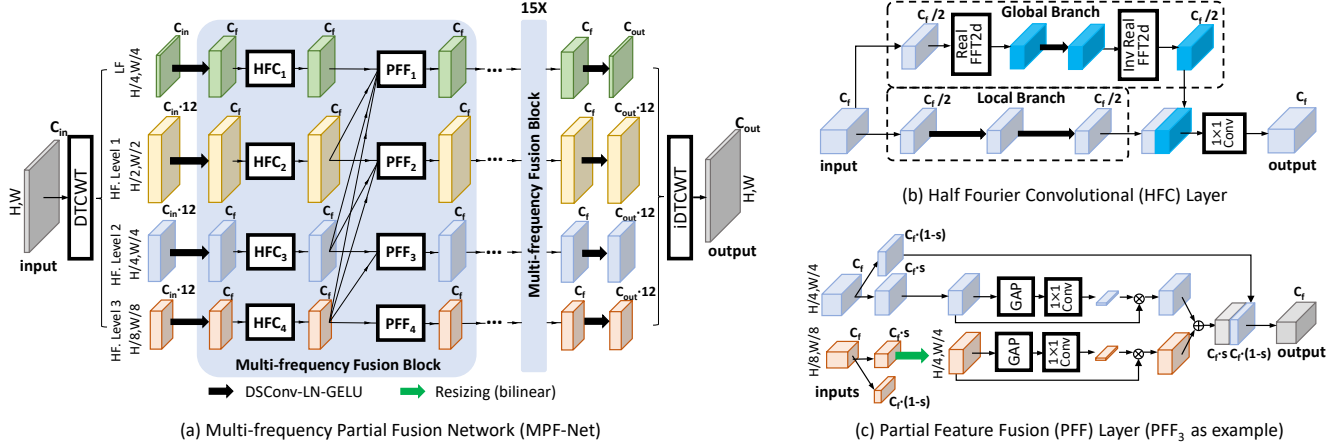


Figure 4. **Network design of Multi-frequency Partial fusion Network (MPF-Net).** It decomposes the input into multi-level subbands and during cross-frequency feature fusion, we preserve a proportion of features learned in the current layer. $C_{in} = C_{out} = 3$ and $C_f = 32$.

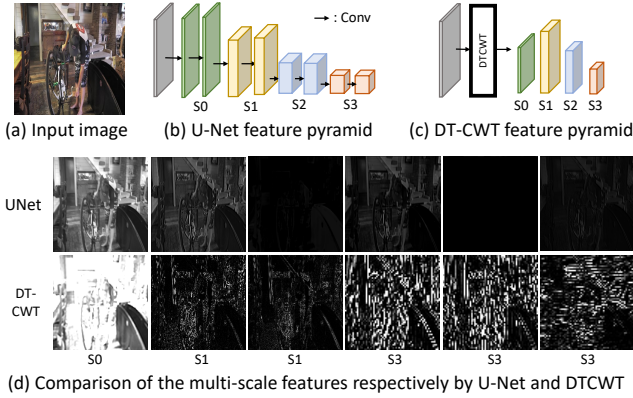


Figure 5. **Illustration of feature mining respectively using DT-CWT transform and U-Net.** DT-CWT requires fewer *Conv* layers yet the generated features show less redundancy or repetition.

3.2. Multi-frequency Partial Fusion Network

In order to combat sophisticated image manipulation within resource-limited environments such as cellphones and cameras, it is essential to deploy a lightweight architecture yet with rich feature extraction capabilities. Fig. 4 illustrates the network design, where we first use a three-level DT-CWT transform to decompose the input into a low-frequency main component and three levels of higher-frequency subbands. Each level consists of six subbands in complex forms, representing different degrees of wavelet information. The real and imaginary parts of the subbands are then concatenated. In Fig. 5, we compare the feature pyramid of U-Net to that of DT-CWT. Vanilla convolutions can be less efficient due to the restriction of receptive field, feature redundancy, and repetition during training. In contrast, DT-CWT provides a strong prior for mitigating these issues, requiring only one layer of separable convolution and yielding richer patterns within representations.

Following the initial feature extraction, we apply a “DSConv-LN-GELU” layer to further refine the extracted features, which is in short for depth-wise separable convolution [30], Layer Normalization [5] and GELU activation [28]. Next, we cascade sixteen multi-frequency partial fusion blocks in each level as feature refinement and fusion. Each block contains a Half Fourier Convolution (HFC) layer and a Partial Feature Fusion (PFF) layer. Notably, these blocks do not alter either the resolution or channel number of the features. Then we project the features back into the main components and three levels of subbands using another “DSConv-LN-GELU” layer, which are then transformed back into the RGB domain via iDT-CWT.

Half Fourier Convolution Layer (HFC). We observe that features provided by DT-CWT provide a rich local pattern, whereas the global information representation is lacking. Considering that Fast Fourier Transform (FFT) is efficient in giving global information about the frequency components of an image [98, 41], we include both vanilla *Conv* layer and Fast Fourier Transform (FFT) in each HFC to enable simultaneous global and local feature mining. For the HFC layer at level i :

$$HFC_i : output = [GB(input_1), LB(input_2)], \quad (4)$$

$$input = [input_1, input_2],$$

where we evenly split the input tensor by half, send them respectively into the Global Branch (GB) and Local Branch (LB) of the HFC layer, and concatenate the resultant features. GB contains FFT, *Conv* layer and inverse FFT. LB is composed of a cascade of two vanilla *Conv* layers.

Partial Feature Fusion Layer (PFF). On fusing different groups of features, two most commonly-accepted ways are “concatenate-and-reduce” [14, 65] or “attend-to-aggregate” [25, 88]. We propose a novel paradigm of “reserve-attend-and-assemble”. Specifically, we split the

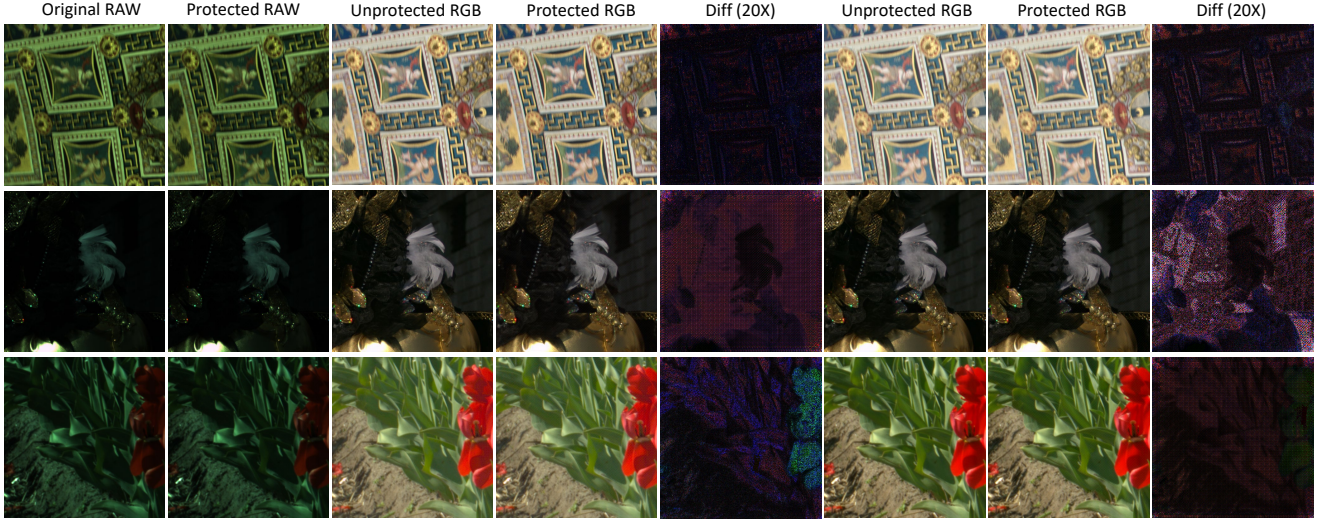


Figure 6. **Examples of protected images under different ISPs.** Dataset: RAISE. In each test, we apply two ISPs for rendering (upper: LibRAW / OpenISP, middle: InvISP / CycleISP, lower: OpenISP / InvISP). The RAW images are visualized through bilinear demosaicing.

input features into two halves based on a predetermined ratio s (default 0.25), i.e., $input_i = [input_{i,1}, input_{i,2}]$ for PFF at level i . The first half of the multi-level features ($C_f \cdot s$) are resized into the size of the current level, and then separately reweighed using channel attention (CA). Next, “assemble” is done by pixel-wisely aggregating all groups of reweighed features and concatenating them with the reserved second half ($C_f \cdot (1 - s)$). Our paradigm can potentially mitigate the issue of over-attention on certain frequencies or covariance drift of the preserved representation, especially from shallow layers, caused by residual learning. Furthermore, we only pass higher-frequency subbands into lower levels, which also encourages each level to process unique combinations of frequencies which reduces redundancy. The operations in PFF at level i can be mathematically defined as follows.

$$PFF_i : output = [input_{i,2}, \sum_{j \leq i} CA(Resize(input_{j,1}))] \quad (5)$$

where CA is composed of a global average pooling layer and a 1×1 bottleneck convolution.

4. Experiments

4.1. Experimental Setups

We use RAISE [15] dataset (8156 image pairs) and Canon subset (2997 image pairs) from the FiveK [9] dataset as the training set. Meanwhile, RAISE, Canon subset and Nikon subset (1600 image pairs) from FiveK as well as SIDD dataset [3] are used to evaluate DRAW. We divide them into training sets and test sets at a ratio of 85:15. We crop each RAW image into non-overlapping sub-images sized 512×512 . For quantitative analysis, inspired

Table 1. **Quantitative analysis on the imperceptibility of RAW protection.** $[R, \hat{R}]$: RAW file before and after protection. $[I, \hat{I}]$: RGB file rendered respectively from R and \hat{R} using different ISP pipelines. Dataset: RAISE and Canon.

Process	512×512		256×256		1024×1024	
	PSNR	SSIM	PSNR	SSIM	PSNR	SSIM
$[R, \hat{R}]$	58.43	-	61.67	-	56.41	-
$[I, \hat{I}]$ (InvISP)	45.13	0.977	46.20	0.985	45.60	0.983
$[I, \hat{I}]$ (LibRaw)	41.25	0.960	41.97	0.967	41.07	0.957
$[I, \hat{I}]$ (Restormer)	45.75	0.980	46.24	0.984	45.03	0.977
$[I, \hat{I}]$ (OpenISP)	40.52	0.960	41.95	0.966	40.34	0.955

by [97, 75], we opt to arbitrarily select regions for copy-moving and inpainting and borrow segmentation masks and the sources from MS-COCO [48] dataset for splicing. For qualitative analysis, we also manually manipulate over one hundred protected images and show some of the representative examples in the figures.

We train our benchmark model by jointly training \mathcal{P} with HRNet [65] as \mathcal{D} . We then fix \mathcal{P} and respectively training MVSS [12] and RIML [75] as \mathcal{D} on top of the protected RGB images. All models are trained with batch size 16 on four distributed NVIDIA RTX 3090 GPUs, and we train the networks for 10 epochs in roughly one day. For gradient descent, we use Adam optimizer with the default hyper-parameters. The learning rate is 1×10^{-4} .

4.2. Performances

Image Quality Assessment. Fig. 6 and Table 1 respectively show the qualitative and quantitative results on the imperceptibility of the protection. Besides, we test the overall image quality of protected images using untrained ISP network, namely, Restormer [86], and another conventional ISP, namely, OpenISP [2]. Restormer is originally proposed

Table 2. **Average performance of different methods on forgery localization.** Dataset: RAISE. The best performances are highlighted in bold type. *: open-source pretrained models finetuned on original RAISE images with *copy-moving*, *splicing* and *inpainting*.

	Models	No attack			Rescaling			AWGN			JPEG90			JPEG70			Med. Blur			GBlur		
		Rec.	F1	IoU																		
<i>splicing</i>	MVSS*	.908	.725	.597	.715	.609	.470	.954	.688	.547	.944	.627	.481	.915	.565	.415	.869	.695	.561	.181	.211	.138
	RIML*	.941	.949	.908	.732	.795	.702	.900	.918	.863	.869	.892	.821	.777	.818	.721	.900	.918	.857	.096	.142	.094
	DRAW-MVSS	.867	.874	.793	.553	.636	.514	.886	.854	.764	.878	.856	.767	.820	.789	.680	.732	.770	.658	.320	.419	.301
	DRAW-RIML	.897	.926	.876	.877	.910	.856	.928	.946	.905	.913	.932	.884	.889	.909	.849	.917	.939	.893	.556	.639	.544
	DRAW-HRNet	.936	.947	.903	.922	.934	.884	.929	.934	.883	.933	.935	.885	.902	.861	.776	.927	.940	.891	.552	.638	.523
<i>copy-moving</i>	MVSS*	.833	.781	.703	.677	.636	.544	.861	.755	.668	.771	.627	.527	.653	.471	.366	.795	.731	.640	.339	.336	.258
	RIML*	.888	.889	.856	.774	.793	.737	.896	.895	.861	.829	.835	.788	.694	.719	.657	.850	.856	.811	.557	.572	.493
	DRAW-MVSS	.901	.893	.857	.839	.836	.780	.915	.890	.850	.862	.842	.793	.804	.767	.706	.871	.851	.803	.631	.657	.582
	DRAW-RIML	.915	.925	.910	.875	.895	.868	.906	.918	.899	.884	.899	.874	.845	.866	.829	.897	.910	.888	.774	.811	.768
	DRAW-HRNet	.969	.970	.959	.960	.956	.937	.962	.957	.943	.955	.951	.932	.916	.884	.839	.958	.955	.939	.915	.920	.885
<i>inpainting</i>	MVSS*	.259	.229	.172	.101	.062	.039	.404	.360	.263	.180	.090	.054	.212	.097	.058	.088	.050	.030	.085	.043	.026
	RIML*	.126	.140	.097	.035	.047	.030	.132	.155	.113	.014	.020	.013	.001	.001	.001	.037	.043	.026	.068	.077	.048
	DRAW-MVSS	.737	.752	.672	.657	.682	.588	.771	.756	.667	.617	.645	.546	.515	.536	.434	.567	.595	.497	.514	.561	.463
	DRAW-RIML	.663	.716	.656	.457	.518	.452	.667	.718	.654	.348	.411	.342	.091	.121	.089	.366	.423	.360	.284	.338	.281
	DRAW-HRNet	.776	.791	.735	.754	.760	.685	.788	.771	.697	.719	.714	.625	.468	.454	.346	.732	.735	.647	.686	.704	.618

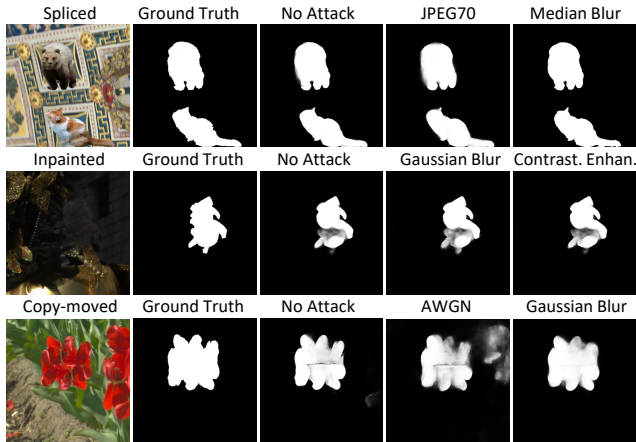


Figure 7. **Exemplified forgery localization results of DRAW-HRNet.** The corresponding protected images are in Fig. 6.

for image restoration, but we find that the transformer-based architecture also shows excellent performance on RGB image rendering. OpenISP is another popular open-source ISP pipeline apart from LibRaw, and we customize the pipeline by applying the most essential modules. We can observe little artifact from the protected version of RAW data and RGB. From the augmented difference, DRAW imperceptibly introduce content-related local patterns, which function like digital *locks* onto the pixels and forgery localization is conducted by observing the integrity of these *locks*.

Robustness and Accuracy of Manipulation Localization.

We conduct comprehensive experiments on RAISE and Canon datasets under different lossy operations. The qualitative and quantitative comparisons in terms of the Recall, F1 and IoU in the pixel domain are reported in Fig. 7, Fig. 8, Table 2 and Table 3. The results under image color adjustment operations and combined attacks are included in the supplement. We find that for DRAW-HRNet, although the images are manipulated by diverse lossy operations, we suc-

Table 3. **Average performance of different methods on forgery localization.** Dataset: CANON.

	Models	No attack		Rescaling		JPEG70		GBlur	
		F1	IoU	F1	IoU	F1	IoU	F1	IoU
<i>splicing</i>	MVSS*	.610	.465	.530	.390	.503	.354	.210	.135
	RIML*	.925	.872	.716	.609	.783	.675	.136	.094
	DRAW-MVSS	.841	.738	.875	.789	.842	.739	.829	.731
	DRAW-RIML	.887	.818	.925	.870	.855	.769	.906	.843
	DRAW-HRNet	.926	.869	.939	.889	.921	.861	.939	.891
<i>copy-moving</i>	MVSS*	.727	.628	.624	.526	.455	.341	.371	.283
	RIML*	.892	.852	.789	.733	.702	.619	.569	.494
	DRAW-MVSS	.912	.879	.868	.828	.832	.785	.826	.776
	DRAW-RIML	.969	.957	.962	.947	.911	.882	.952	.933
	DRAW-HRNet	.968	.956	.960	.945	.922	.895	.952	.934
<i>inpainting</i>	MVSS*	.215	.150	.100	.064	.136	.083	.073	.045
	RIML*	.102	.070	.033	.021	.003	.001	.012	.007
	DRAW-MVSS	.829	.753	.676	.574	.115	.076	.513	.407
	DRAW-RIML	.949	.918	.889	.836	.406	.326	.849	.784
	DRAW-HRNet	.934	.894	.867	.811	.360	.284	.761	.691

ceed in localizing the tampered areas. If there are no lossy operations, the F1 scores are in most cases above 0.8. Fig. 7 further provides exemplified image manipulation localization results of DRAW-HRNet under different lossy operations.

Next, for fair comparison with previous arts, we fine-tune MVSS and RIML on RAISE and Canon dataset using the mechanisms proposed in the corresponding papers yet additionally considering *splicing*, *copy-moving* and *inpainting*. When heavy image lossy operations are present, MVSS fails to detect the tampered content. While RIML exhibits better robustness due to OSN transmission simulation, its performances under blurring or inpainting attacks are still restricted. However, training these detectors based on the protected images significantly improves their robustness.

Generalizability. We conduct additional experiments where \mathcal{P} trained on RAISE dataset is applied on different RAW datasets, i.e., Canon and SIDD, and untrained ISP pipelines, i.e., OpenISP and Restormer. Table 4 shows that raw protection can generalize to untrained cameras and ISP

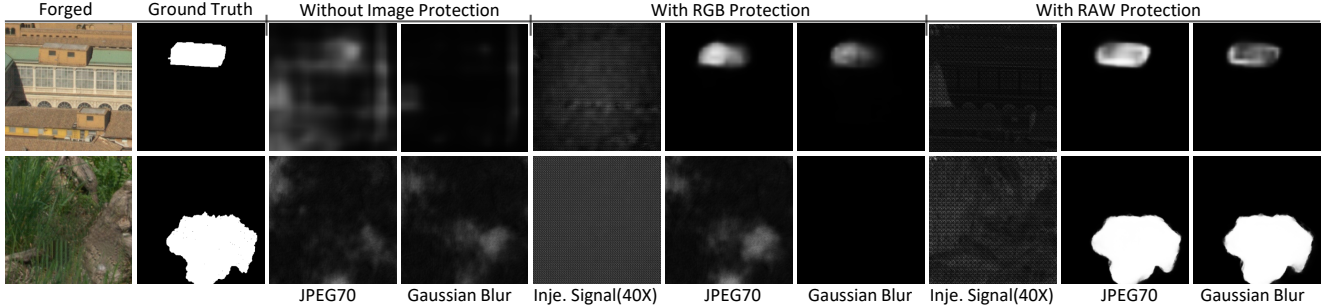


Figure 8. **Qualitative analysis on performance between passive localization without image protection, with RGB protection and with RAW protection.** Dataset: RAISE. \mathcal{D} : MVSS* (upper), RIML* (lower). Type: copy-moving (upper), inpainting (lower).

Table 4. **Generalizability to untrained ISP pipelines or datasets.** \mathcal{P} and \mathcal{D} are trained on RAISE.

Test Item		Forgery	NoAtk	Rescale	JPEG70	M-Blur	G-Blur
ISP	OpenISP	Spli.	.929	.910	.837	.933	.620
		Copy.	.941	.919	.843	.941	.880
		Inpa.	.850	.820	.451	.765	.756
	Restormer	Spli.	.946	.936	.863	.941	.648
		Copy.	.961	.947	.871	.948	.904
		Inpa.	.906	.833	.487	.789	.759
Dataset	Canon	Spli.	.936	.925	.845	.931	.596
		Copy.	.957	.930	.859	.946	.881
		Inpa.	.805	.732	.486	.710	.706
	SIDD	Spli.	.928	.909	.832	.911	.574
		Copy.	.967	.965	.891	.954	.880
		Inpa.	.686	.628	.400	.574	.554

Table 5. **Generalizability to lossy transmission and untrained perturbations.** Dataset: RAISE.

Forgery	S&P		Dual JPEG		Facebook		Weibo		WeChat	
	F1	IoU	F1	IoU	F1	IoU	F1	IoU	F1	IoU
splicing	.839	.855	.657	.683	.917	.920	.902	.897	.763	.728
copymove	.854	.850	.692	.729	.905	.910	.859	.870	.637	.688
inpainting	.687	.711	.377	.423	.665	.598	.623	.577	.410	.355

Table 6. **Comparison of computational cost** among lightweight image-to-image-translation or segmentation networks.

	SegNet [6]	ShuffleNet [52]	U-Net [58]	ENet [54]	MPF-Net
Params	29.5M	0.94M	26.35M	0.36M	0.25M
FLOPS	0.56T	22.9G	0.22T	2.34G	7.39G
Memory	465MB	390MB	767MB	46MB	160MB

pipelines while preserving promising detection capacity.

To justify the generalizability to lossy transmission, we randomly handcraft 150 manipulated images, upload them onto several famous OSNs and download them for detection. Also, we test the performance against dual JPEG and salt & pepper attack ($p = 5\%$) which are untrained types for DRAW. As shown in Table 5, DRAW can effectively resist lossy OSN transmission, and its protection remains valuable against unknown lossy operations.

Computational Complexity. We compare the computational requirements of MPF-Net in Table 6 with SegNet [6], ShuffleNet [52], U-Net [58] and ENet [54], which are famous lightweight models for image segmentation. MPF-Net requires lower computing resources, e.g. only 20.9% in memory cost and 0.95% in parameters compared to the classical U-Net.

4.3. Baseline Comparisons

Previous techniques in proactive image forgery detection, e.g., tag retrieval [71] or template matching [4], are not suitable for image manipulation localization. Moreover, Ying et al. [83]’s method additionally considers image self-recovery, which inevitably includes much heavier protective signal. Therefore, we alternatively build two baseline methods that respectively apply pure robust training using our proposed attack layer and apply RGB-domain protection. In

the tests, MVSS is employed as localization network. The quantitative comparison results are reported in Table 7. Further details regarding the experimental settings for the two baseline methods are included in the supplement.

RAW Protection vs Pure Robust Training. Our proposed robust training mechanism reflected in the attack layer is different from that proposed in RIML. Specifically, we render the unprotected RAW files \mathbf{R} using \mathcal{S} , which are then attacked by \mathcal{A} . We see that the introduction of robust training can help boost the performance of MVSS. However, the overall performance is still worse than further applying RAW protection to aid localization. In severe degrading cases such as blurring, the performance gap between RAW protection and robust training without protection regarding F1 score is more than ten percent.

RAW protection vs RGB protection. For fair comparison, we regulate that the overall PSNR on RGB images before and after RGB protection should be above 40 dB, in line with the criterion in Table 1. We conduct qualitative experiment in Fig 8 to evaluate the effectiveness of image protection. According to the experimental results, RGB protection cannot aid robust manipulation localization if the magnitude of RGB modification is restricted. We also grayscale the augmented injected signal for better visualization and found that signal injected by RAW protection is more adaptive in magnitude to the image contents. One pos-

Table 7. Comparison with baseline methods on RAISE.

We verify the importance of RAW protection by comparing the results with those of pure robust training using \mathcal{A} and direct RGB protection. \mathcal{P}^- : using \mathcal{P} for RGB protection. \mathcal{D} : MVSS*

	Used Modules				Rescaling		JPEG70		Med. Blur		GBLur	
	\mathcal{P}	\mathcal{P}^-	\mathcal{A}	\mathcal{D}	F1	IoU	F1	IoU	F1	IoU	F1	IoU
splicing			✓	✓	.609	.470	.565	.415	.695	.561	.211	.138
			✓	✓	.668	.534	.725	.590	.762	.635	.303	.207
	✓	✓	✓	✓	.358	.253	.438	.317	.487	.361	.149	.097
inpainting			✓	✓	.636	.514	.789	.680	.770	.658	.419	.301
			✓	✓	.636	.544	.471	.366	.731	.640	.336	.258
		✓	✓	✓	.859	.816	.648	.582	.782	.728	.528	.456
copy-moving			✓	✓	.490	.412	.467	.382	.626	.548	.268	.208
		✓	✓	✓	.836	.780	.767	.706	.851	.803	.657	.582
	✓	✓	✓	✓	.062	.039	.097	.058	.050	.030	.043	.026
inpainting			✓	✓	.605	.494	.231	.159	.398	.297	.342	.249
		✓	✓	✓	.387	.291	.480	.371	.381	.288	.374	.279
	✓	✓	✓	✓	.682	.588	.536	.434	.595	.497	.561	.463

sible reason is that the densely-predicting task requires hiding more information than binary image forgery classification task, making it struggle to maintain high fidelity of the original image. In comparison, RAW protection can adaptively introduce protection with the help of content-related procedures, e.g., demosaicing and noise reduction, within the subsequent ISP algorithms that suppress unwanted artifacts and biases. Theoretically, RAW data modification enjoys a much larger search space that allows transformations from the original image into another image with high density upon sampling.

4.4. Ablation Studies

Table 8 and Fig. 9 respectively show the quantitative and qualitative results of ablation studies. In each test, we regulate that the averaged PSNR between \mathbf{I} and $\hat{\mathbf{I}}$, with ISP pipelines evenly applied, should be within the range of 41-43 dB, to ensure imperceptible image protection.

Substituting the architecture of \mathcal{P} . We first test if using U-Net with a similar amount of parameters or ENet [54] as \mathcal{P} can achieve similar performance on splicing detection. First, though ENet contains similar amount of parameters compared to MPF-Net, the performance of image manipulation localization using ENet as \mathcal{P} is not satisfactory. Second, though U-Net with *DSC* provides much better result, because the channel numbers within each layer are restricted within 48 to save computational complexity, the performance is still worse than our benchmark.

Impact of components in MPF-Net. The most noticeable difference between MPFNet with previous U-shaped networks is that feature disentanglement can be better ensured even with fewer parameters. To verify this, we respectively replace the HFC layer and PFF layer with typical alternatives, i.e., vanilla convolution and channel-wise concatenation. The performances are nearly 5-10 points weaker compared to the MPF-Net setup. First, DT-CWT is a shift-invariant wavelet transform that comes with limited redun-

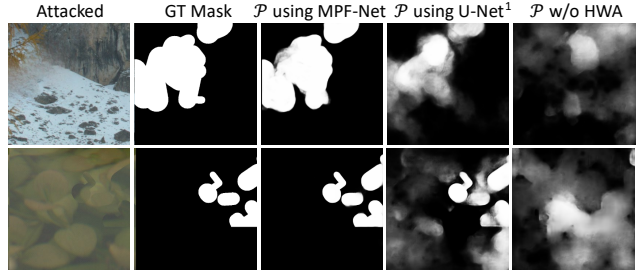


Figure 9. Examples of ablation studies of DRAW. We observe that either replacing MPF-Net with U-Net using *DSC* or removing HFC module results in decreased performance. Upper: inpainting + JPEG80. Lower: copy-moving + median-blur.

Table 8. Ablation study on DRAW on Nikon using splicing attack. ¹: replacing *Conv* layers with *DSC*.

Test	F1		
	NoAtk	JPEG70	Mblur
\mathcal{P} using U-Net ¹	.877	.769	.535
\mathcal{P} using ENet	.324	.137	.092
MPF-Net w/o HFC	.844	.710	.602
MPF-Net w/o DT-CWT	.852	.751	.626
MPF-Net w/o PFF	.827	.712	.667
w/o diff from real attack	.842	.566	.502
using only one ISP Surrogate	.648	.455	.267
w/o Image Distortion Module	.929	.245	.116
w/o Color Adjustment Module	.814	.759	.641
Full implementation of DRAW	.929	.838	.696

dancy. Second, partial feature fusion and partial connection are more flexible. The design explicitly keeps some of the features extracted from the current level and directly feeds them into the subsequent block. Therefore, for different levels, the input features will be different, which encourages feature disentanglement.

Impact of pipeline design. We also tested the setting of not using the image distortion module or color adjustment module in the pipeline during training. The result is as expected that the scheme will therefore lack generalizability in overall robustness due to the fact that there are not enough random processes that can simulate the real-world situation. Besides, not introducing the difference between the real-world and simulated attacks or using only one ISP surrogate model will also impair the overall performance.

5. Conclusions

We present DRAW that adds imperceptible protective signal to the RAW data against image manipulation. The protection can be transferred into RGB images and resist lossy operations. Extensive experiments on typical RAW datasets prove the effectiveness of DRAW.

Acknowledgment. This work was supported by National Natural Science Foundation of China under Grant U20B2051, U1936214, U22B2047, 62072114 and U20A20178.

References

- [1] Libraw: Library for reading and processing of raw digicam images. <https://github.com/LibRaw/LibRaw>. 3
- [2] Openisp. <https://github.com/mushfiqulalam/isp>. 3, 5
- [3] Abdelrahman Abdelhamed, Stephen Lin, and Michael S. Brown. A high-quality denoising dataset for smartphone cameras. In *IEEE Conference on Computer Vision and Pattern Recognition (CVPR)*, June 2018. 5
- [4] Vishal Asnani, Xi Yin, Tal Hassner, Sijia Liu, and Xiaoming Liu. Proactive image manipulation detection. In *Proceedings of the IEEE/CVF Conference on Computer Vision and Pattern Recognition*, pages 15386–15395, 2022. 2, 7
- [5] Jimmy Lei Ba, Jamie Ryan Kiros, and Geoffrey E Hinton. Layer normalization. *arXiv preprint arXiv:1607.06450*, 2016. 4
- [6] Vijay Badrinarayanan, Alex Kendall, and Roberto Cipolla. Segnet: A deep convolutional encoder-decoder architecture for image segmentation. *IEEE transactions on pattern analysis and machine intelligence*, 39(12):2481–2495, 2017. 2, 7
- [7] Yoshua Bengio, Nicholas Léonard, and Aaron Courville. Estimating or propagating gradients through stochastic neurons for conditional computation. *arXiv preprint arXiv:1308.3432*, 2013. 3
- [8] Vladimir Bychkovsky, Sylvain Paris, Eric Chan, and Frédo Durand. Learning photographic global tonal adjustment with a database of input / output image pairs. In *The Twenty-Fourth IEEE Conference on Computer Vision and Pattern Recognition*, 2011.
- [9] Vladimir Bychkovsky, Sylvain Paris, Eric Chan, and Frédo Durand. Learning photographic global tonal adjustment with a database of input/output image pairs. In *CVPR 2011*, pages 97–104. IEEE, 2011. 5
- [10] Keshigeyan Chandrasegaran, Ngoc-Trung Tran, and Ngai-Man Cheung. A closer look at fourier spectrum discrepancies for cnn-generated images detection. In *Proceedings of the IEEE/CVF conference on computer vision and pattern recognition*, pages 7200–7209, 2021.
- [11] Mo Chen, Jessica Fridrich, Miroslav Goljan, and Jan Lukás. Determining image origin and integrity using sensor noise. *IEEE Transactions on information forensics and security*, 3(1):74–90, 2008. 1
- [12] Xinru Chen, Chengbo Dong, Jiaqi Ji, Juan Cao, and Xirong Li. Image manipulation detection by multi-view multi-scale supervision. In *Proceedings of the IEEE/CVF International Conference on Computer Vision (ICCV)*, pages 14185–14193, 2021. 1, 2, 3, 5
- [13] Yunpeng Chen, Haoqi Fan, Bing Xu, Zhicheng Yan, Yanis Kalantidis, Marcus Rohrbach, Shuicheng Yan, and Jiashi Feng. Drop an octave: Reducing spatial redundancy in convolutional neural networks with octave convolution. In *Proceedings of the IEEE/CVF International Conference on Computer Vision*, pages 3435–3444, 2019.
- [14] Sung-Jin Cho, Seo-Won Ji, Jun-Pyo Hong, Seung-Won Jung, and Sung-Jea Ko. Rethinking coarse-to-fine approach in single image deblurring. In *Proceedings of the IEEE/CVF international conference on computer vision*, pages 4641–4650, 2021. 4
- [15] Duc-Tien Dang-Nguyen, Cecilia Pasquini, Valentina Conotter, and Giulia Boato. Raise: A raw images dataset for digital image forensics. In *Proceedings of the 6th ACM multimedia systems conference*, pages 219–224, 2015. 5
- [16] Laurent Dinh, David Krueger, and Yoshua Bengio. Nice: Non-linear independent components estimation. *arXiv preprint arXiv:1410.8516*, 2014.
- [17] Laurent Dinh, Jascha Sohl-Dickstein, and Samy Bengio. Density estimation using real nvp. *arXiv preprint arXiv:1605.08803*, 2016.
- [18] Jing Dong, Wei Wang, and Tieniu Tan. Casia image tampering detection evaluation database. In *2013 IEEE China Summit and International Conference on Signal and Information Processing*, pages 422–426. IEEE, 2013.
- [19] Qiaole Dong, Chenjie Cao, and Yanwei Fu. Incremental transformer structure enhanced image inpainting with masking positional encoding. In *Proceedings of the IEEE/CVF Conference on Computer Vision and Pattern Recognition*, pages 11358–11368, 2022. 1
- [20] Tarik Dzanic, Karan Shah, and Freddie Witherden. Fourier spectrum discrepancies in deep network generated images. *Advances in neural information processing systems*, 33:3022–3032, 2020.
- [21] Ilya Eckstein, James Patrick Lee-Thorp, Joshua Ainslie, and Santiago Ontanon. Fnet: Mixing tokens with fourier transforms. 2022.
- [22] Patrick Esser, Robin Rombach, and Bjorn Ommer. Taming transformers for high-resolution image synthesis. In *Proceedings of the IEEE/CVF conference on computer vision and pattern recognition*, pages 12873–12883, 2021.
- [23] Pasquale Ferrara, Tiziano Bianchi, Alessia De Rosa, and Alessandro Piva. Image forgery localization via fine-grained analysis of cfa artifacts. *IEEE Transactions on Information Forensics and Security*, 7(5):1566–1577, 2012.
- [24] Jessica Fridrich and Jan Kodovsky. Rich models for steganalysis of digital images. *IEEE Transactions on information forensics and security*, 7(3):868–882, 2012. 2
- [25] Jun Fu, Jing Liu, Haijie Tian, Yong Li, Yongjun Bao, Zhiwei Fang, and Hanqing Lu. Dual attention network for scene segmentation. In *Proceedings of the IEEE/CVF conference on computer vision and pattern recognition*, pages 3146–3154, 2019. 4
- [26] Robert Geirhos, Jörn-Henrik Jacobsen, Claudio Michaelis, Richard Zemel, Wieland Brendel, Matthias Bethge, and Felix A Wichmann. Shortcut learning in deep neural networks. *Nature Machine Intelligence*, 2(11):665–673, 2020.
- [27] Felix Heide, Markus Steinberger, Yun-Ta Tsai, Mushfiqur Rouf, Dawid Pająk, Dikpal Reddy, Orazio Gallo, Jing Liu, Wolfgang Heidrich, Karen Egiazarian, et al. Flexisp: A flexible camera image processing framework. *ACM Transactions on Graphics (ToG)*, 33(6):1–13, 2014.
- [28] Dan Hendrycks and Kevin Gimpel. Gaussian error linear units (gelus). *arXiv preprint arXiv:1606.08415*, 2016. 4
- [29] Paul Hill, Alin Achim, and David Bull. The undecimated dual tree complex wavelet transform and its application to

- bivariate image denoising using a cauchy model. In *2012 19th IEEE international conference on image processing*, pages 1205–1208. IEEE, 2012.
- [30] Andrew G Howard, Menglong Zhu, Bo Chen, Dmitry Kalenichenko, Weijun Wang, Tobias Weyand, Marco Andreetto, and Hartwig Adam. Mobilenets: Efficient convolutional neural networks for mobile vision applications. *arXiv preprint arXiv:1704.04861*, 2017. 2, 4
- [31] Jie Hu, Li Shen, and Gang Sun. Squeeze-and-excitation networks. In *Proceedings of the IEEE conference on computer vision and pattern recognition*, pages 7132–7141, 2018.
- [32] Xuefeng Hu, Zhihan Zhang, Zhenye Jiang, Syomantak Chaudhuri, Zhenheng Yang, and Ram Nevatia. Span: Spatial pyramid attention network for image manipulation localization. In *European Conference on Computer Vision (ECCV)*, pages 312–328. Springer, 2020. 1, 2
- [33] Ashraful Islam, Chengjiang Long, Arslan Basharat, and Anthony Hoogs. Doa-gan: Dual-order attentive generative adversarial network for image copy-move forgery detection and localization. In *Proceedings of the IEEE/CVF Conference on Computer Vision and Pattern Recognition (CVPR)*, pages 4676–4685, 2020. 2
- [34] Sara Izadpanahi and Hasan Demirel. Motion based video super resolution using edge directed interpolation and complex wavelet transform. *Signal Processing*, 93(7):2076–2086, 2013.
- [35] Junpeng Jing, Xin Deng, Mai Xu, Jianyi Wang, and Zhenyu Guan. Hinet: Deep image hiding by invertible network. In *Proceedings of the IEEE/CVF International Conference on Computer Vision*, pages 4733–4742, 2021. 2
- [36] Justin Johnson, Alexandre Alahi, and Li Fei-Fei. Perceptual losses for real-time style transfer and super-resolution. In *European Conference on Computer Vision (ECCV)*, pages 694–711. Springer, 2016.
- [37] David Khachaturov, Iliia Shumailov, Yiren Zhao, Nicolas Papernot, and Ross Anderson. Markpainting: Adversarial machine learning meets inpainting. In *International Conference on Machine Learning (ICML)*, pages 5409–5419, 2021. 2
- [38] Durk P Kingma and Prafulla Dhariwal. Glow: Generative flow with invertible 1x1 convolutions. *Advances in neural information processing systems*, 31, 2018.
- [39] Kenji Kurosawa, Kenro Kuroki, and Naoki Saitoh. Ccd fingerprint method-identification of a video camera from videotaped images. In *Proceedings 1999 International Conference on Image Processing (Cat. 99CH36348)*, volume 3, pages 537–540. IEEE, 1999. 1
- [40] Myung-Joon Kwon, Seung-Hun Nam, In-Jae Yu, Heung-Kyu Lee, and Changick Kim. Learning jpeg compression artifacts for image manipulation detection and localization. *International Journal of Computer Vision*, pages 1–21, 2022.
- [41] James Lee-Thorp, Joshua Ainslie, Ilya Eckstein, and Santiago Ontanon. Fnet: Mixing tokens with fourier transforms. *arXiv preprint arXiv:2105.03824*, 2021. 4
- [42] Haodong Li and Jiwu Huang. Localization of deep inpainting using high-pass fully convolutional network. In *Proceedings of the IEEE/CVF International Conference on Computer Vision (ICCV)*, pages 8301–8310, 2019. 2
- [43] Jiaming Li, Hongtao Xie, Jiahong Li, Zhongyuan Wang, and Yongdong Zhang. Frequency-aware discriminative feature learning supervised by single-center loss for face forgery detection. In *Proceedings of the IEEE/CVF conference on computer vision and pattern recognition*, pages 6458–6467, 2021.
- [44] Ying Li, Yu Wang, Tuo Leng, and Wen Zhijie. Wavelet u-net for medical image segmentation. In *Artificial Neural Networks and Machine Learning–ICANN 2020: 29th International Conference on Artificial Neural Networks, Bratislava, Slovakia, September 15–18, 2020, Proceedings, Part I 29*, pages 800–810. Springer, 2020.
- [45] Yuanman Li and Jiantao Zhou. Fast and effective image copy-move forgery detection via hierarchical feature point matching. *IEEE Transactions on Information Forensics and Security (TIFS)*, 14(5):1307–1322, 2018. 2
- [46] Zhetong Liang, Jianrui Cai, Zisheng Cao, and Lei Zhang. Cameranet: A two-stage framework for effective camera isp learning. *IEEE Transactions on Image Processing*, 30:2248–2262, 2021.
- [47] Tsung-Yi Lin, Piotr Dollár, Ross Girshick, Kaiming He, Bharath Hariharan, and Serge Belongie. Feature pyramid networks for object detection. In *Proceedings of the IEEE conference on computer vision and pattern recognition*, pages 2117–2125, 2017. 2
- [48] Tsung-Yi Lin, Michael Maire, Serge Belongie, James Hays, Pietro Perona, Deva Ramanan, Piotr Dollár, and C Lawrence Zitnick. Microsoft coco: Common objects in context. In *European conference on computer vision*, pages 740–755. Springer, 2014. 5
- [49] Yuzhen Lin, Han Chen, Emanuele Maiorana, Patrizio Campisi, and Bin Li. Source-id-tracker: Source face identity protection in face swapping. In *2022 IEEE International Conference on Multimedia and Expo (ICME)*, pages 01–06. IEEE, 2022.
- [50] Honggu Liu, Xiaodan Li, Wenbo Zhou, Yuefeng Chen, Yuan He, Hui Xue, Weiming Zhang, and Nenghai Yu. Spatial-phase shallow learning: rethinking face forgery detection in frequency domain. In *Proceedings of the IEEE/CVF conference on computer vision and pattern recognition*, pages 772–781, 2021.
- [51] Shao-Ping Lu, Rong Wang, Tao Zhong, and Paul L Rosin. Large-capacity image steganography based on invertible neural networks. In *Proceedings of the IEEE/CVF Conference on Computer Vision and Pattern Recognition (CVPR)*, pages 10816–10825, 2021. 2
- [52] Ningning Ma, Xiangyu Zhang, Hai-Tao Zheng, and Jian Sun. Shufflenet v2: Practical guidelines for efficient cnn architecture design. In *Proceedings of the European conference on computer vision (ECCV)*, pages 116–131, 2018. 2, 7
- [53] Gaël Mahfoudi, Badr Tajini, Florent Reiraint, Frederic Morain-Nicolier, Jean Luc Dugelay, and PIC Marc. Defacto: Image and face manipulation dataset. In *2019 27th European Signal Processing Conference (EUSIPCO)*, pages 1–5. IEEE, 2019.

- [54] Adam Paszke, Abhishek Chaurasia, Sangpil Kim, and Eugenio Culurciello. Enet: A deep neural network architecture for real-time semantic segmentation. *arXiv preprint arXiv:1606.02147*, 2016. **2, 7, 8**
- [55] Alin C Popescu and Hany Farid. Exposing digital forgeries in color filter array interpolated images. *IEEE Transactions on Signal Processing*, 53(10):3948–3959, 2005. **1**
- [56] Yuyang Qian, Guojun Yin, Lu Sheng, Zixuan Chen, and Jing Shao. Thinking in frequency: Face forgery detection by mining frequency-aware clues. In *Computer Vision—ECCV 2020: 16th European Conference, Glasgow, UK, August 23–28, 2020, Proceedings, Part XII*, pages 86–103. Springer, 2020.
- [57] Haotong Qin, Ruihao Gong, Xianglong Liu, Xiao Bai, Jingkuan Song, and Nicu Sebe. Binary neural networks: A survey. *Pattern Recognition*, 105:107281, 2020.
- [58] Olaf Ronneberger, Philipp Fischer, and Thomas Brox. U-net: Convolutional networks for biomedical image segmentation. In *International Conference on Medical Image Computing and Computer-Assisted Intervention (MICCAI)*, pages 234–241. Springer, 2015. **2, 7**
- [59] Ronald Salloum, Yuzhuo Ren, and C-C Jay Kuo. Image splicing localization using a multi-task fully convolutional network (mfcn). *Journal of Visual Communication and Image Representation*, 51:201–209, 2018. **2**
- [60] Eli Schwartz, Raja Giryes, and Alex M Bronstein. Deepisp: Toward learning an end-to-end image processing pipeline. *IEEE Transactions on Image Processing*, 28(2):912–923, 2018.
- [61] Ivan W Selesnick, Richard G Baraniuk, and Nick C Kingsbury. The dual-tree complex wavelet transform. *IEEE signal processing magazine*, 22(6):123–151, 2005.
- [62] Sandeep Singh Sengar and Susanta Mukhopadhyay. Moving object detection using statistical background subtraction in wavelet compressed domain. *Multimedia Tools and Applications*, 79(9-10):5919–5940, 2020.
- [63] Richard Shin and Dawn Song. Jpeg-resistant adversarial images. In *NIPS 2017 Workshop on Machine Learning and Computer Security*, volume 1, 2017.
- [64] Radomir S Stanković and Bogdan J Falkowski. The haar wavelet transform: its status and achievements. *Computers & Electrical Engineering*, 29(1):25–44, 2003.
- [65] Ke Sun, Bin Xiao, Dong Liu, and Jingdong Wang. Deep high-resolution representation learning for human pose estimation. In *Proceedings of the IEEE/CVF conference on computer vision and pattern recognition*, pages 5693–5703, 2019. **3, 4, 5**
- [66] Yue-Hui Sun and Ming-Hui Du. Face detection using dt-cwt on spectral histogram. In *2006 International Conference on Machine Learning and Cybernetics*, pages 3637–3642. IEEE, 2006.
- [67] Roman Suvorov, Elizaveta Logacheva, Anton Mashikhin, Anastasia Remizova, Arsenii Ashukha, Aleksei Silvestrov, Naejin Kong, Harshith Goka, Kiwoong Park, and Victor Lempitsky. Resolution-robust large mask inpainting with fourier convolutions. In *Proceedings of the IEEE/CVF Winter Conference on Applications of Computer Vision*, pages 2149–2159, 2022. **1**
- [68] Aaron Van Den Oord, Oriol Vinyals, et al. Neural discrete representation learning. *Advances in neural information processing systems*, 30, 2017.
- [69] Cédric Vonesch, Thierry Blu, and Michael Unser. Generalized daubechies wavelet families. *IEEE Transactions on Signal Processing*, 55(9):4415–4429, 2007.
- [70] Chien-Yao Wang, Hong-Yuan Mark Liao, Yueh-Hua Wu, Ping-Yang Chen, Jun-Wei Hsieh, and I-Hau Yeh. Cspnet: A new backbone that can enhance learning capability of cnn. In *Proceedings of the IEEE/CVF conference on computer vision and pattern recognition workshops*, pages 390–391, 2020.
- [71] Run Wang, Felix Juefei-Xu, Meng Luo, Yang Liu, and Lina Wang. Faketagger: Robust safeguards against deepfake dissemination via provenance tracking. In *Proceedings of the 29th ACM International Conference on Multimedia*, pages 3546–3555, 2021. **2, 7**
- [72] Sheng-Yu Wang, Oliver Wang, Richard Zhang, Andrew Owens, and Alexei A Efros. Cnn-generated images are surprisingly easy to spot... for now. In *Proceedings of the IEEE/CVF conference on computer vision and pattern recognition*, pages 8695–8704, 2020.
- [73] Yu Wang, Quan Zhou, Jia Liu, Jian Xiong, Guangwei Gao, Xiaofu Wu, and Longin Jan Latecki. Lednet: A lightweight encoder-decoder network for real-time semantic segmentation. In *2019 IEEE International Conference on Image Processing (ICIP)*, pages 1860–1864. IEEE, 2019.
- [74] Zhou Wang, Alan C Bovik, Hamid R Sheikh, and Eero P Simoncelli. Image quality assessment: from error visibility to structural similarity. *IEEE Transactions on Image Processing (TIP)*, 13(4):600–612, 2004.
- [75] Haiwei Wu, Jiantao Zhou, Jinyu Tian, and Jun Liu. Robust image forgery detection over online social network shared images. In *Proceedings of the IEEE/CVF Conference on Computer Vision and Pattern Recognition*, pages 13440–13449, 2022. **1, 2, 3, 5**
- [76] Haiwei Wu, Jiantao Zhou, Jinyu Tian, Jun Liu, and Yu Qiao. Robust image forgery detection against transmission over online social networks. *IEEE Transactions on Information Forensics and Security*, 17:443–456, 2022. **1**
- [77] Yue Wu, Wael AbdAlmageed, and Premkumar Natarajan. Mantra-net: Manipulation tracing network for detection and localization of image forgeries with anomalous features. In *Proceedings of the IEEE/CVF Conference on Computer Vision and Pattern Recognition (CVPR)*, pages 9543–9552, 2019. **1, 2**
- [78] Yazhou Xing, Zian Qian, and Qifeng Chen. Invertible image signal processing. In *Proceedings of the IEEE/CVF Conference on Computer Vision and Pattern Recognition*, pages 6287–6296, 2021. **3**
- [79] Kai Xu, Minghai Qin, Fei Sun, Yuhao Wang, Yen-Kuang Chen, and Fengbo Ren. Learning in the frequency domain. In *Proceedings of the IEEE/CVF Conference on Computer Vision and Pattern Recognition*, pages 1740–1749, 2020.
- [80] Kai Xu, Minghai Qin, Fei Sun, Yuhao Wang, Yen-Kuang Chen, and Fengbo Ren. Learning in the frequency domain. In *Proceedings of the IEEE/CVF Conference on Computer Vision and Pattern Recognition*, pages 1740–1749, 2020.

- [81] Minghao Yin, Yongbing Zhang, Xiu Li, and Shiqi Wang. When deep fool meets deep prior: Adversarial attack on super-resolution network. In *Proceedings of the 26th ACM international conference on Multimedia*, pages 1930–1938, 2018. [2](#)
- [82] Qichao Ying, Jingzhi Lin, Zhenxing Qian, Haisheng Xu, and Xinpeng Zhang. Robust digital watermarking for color images in combined dft and dt-cwt domains. *Mathematical Biosciences and Engineering*, 16(5):4788–4801, 2019. [2](#)
- [83] Qichao Ying, Zhenxing Qian, Hang Zhou, Haisheng Xu, Xinpeng Zhang, and Siyi Li. From image to image: Immunized image generation. In *Proceedings of the 29th ACM international conference on Multimedia*, pages 1–9, 2021. [2](#), [7](#)
- [84] Jiahui Yu, Zhe Lin, Jimei Yang, Xiaohui Shen, Xin Lu, and Thomas S Huang. Generative image inpainting with contextual attention. In *Proceedings of the IEEE/CVF Conference on Computer Vision and Pattern Recognition (CVPR)*, pages 5505–5514, 2018.
- [85] Jiahui Yu, Zhe Lin, Jimei Yang, Xiaohui Shen, Xin Lu, and Thomas S Huang. Free-form image inpainting with gated convolution. In *Proceedings of the IEEE/CVF international conference on computer vision*, pages 4471–4480, 2019.
- [86] Syed Waqas Zamir, Aditya Arora, Salman Khan, Munawar Hayat, Fahad Shahbaz Khan, and Ming-Hsuan Yang. Restormer: Efficient transformer for high-resolution image restoration. In *Proceedings of the IEEE/CVF Conference on Computer Vision and Pattern Recognition*, pages 5728–5739, 2022. [3](#), [5](#)
- [87] Syed Waqas Zamir, Aditya Arora, Salman Khan, Munawar Hayat, Fahad Shahbaz Khan, Ming-Hsuan Yang, and Ling Shao. Cycleisp: Real image restoration via improved data synthesis. In *Proceedings of the IEEE/CVF Conference on Computer Vision and Pattern Recognition*, pages 2696–2705, 2020. [3](#)
- [88] Syed Waqas Zamir, Aditya Arora, Salman Khan, Munawar Hayat, Fahad Shahbaz Khan, Ming-Hsuan Yang, and Ling Shao. Learning enriched features for real image restoration and enhancement. In *Computer Vision—ECCV 2020: 16th European Conference, Glasgow, UK, August 23–28, 2020, Proceedings, Part XXV 16*, pages 492–511. Springer, 2020. [4](#)
- [89] Richard Zhang, Phillip Isola, Alexei A Efros, Eli Shechtman, and Oliver Wang. The unreasonable effectiveness of deep features as a perceptual metric. In *Proceedings of the IEEE conference on computer vision and pattern recognition*, pages 586–595, 2018. [3](#)
- [90] Xinpeng Zhang. Fragile watermarking scheme using a hierarchical mechanism. *Signal processing*, 89(4):675–679, 2009.
- [91] Xuaner Zhang, Qifeng Chen, Ren Ng, and Vladlen Koltun. Zoom to learn, learn to zoom. In *Proceedings of the IEEE/CVF Conference on Computer Vision and Pattern Recognition*, pages 3762–3770, 2019. [3](#)
- [92] Xinpeng Zhang, Zhenxing Qian, and Guorui Feng. Reference sharing mechanism for watermark self-embedding. *IEEE Transactions on Image Processing (TIP)*, 20(2):485–495, 2010.
- [93] Xinpeng Zhang and Shuozhong Wang. Fragile watermarking with error-free restoration capability. *IEEE Transactions on Multimedia*, 10(8):1490–1499, 2008.
- [94] Yuxuan Zhang, Bo Dong, and Felix Heide. All you need is raw: Defending against adversarial attacks with camera image pipelines. *arXiv preprint arXiv:2112.09219*, 2021.
- [95] Hengshuang Zhao, Jianping Shi, Xiaojuan Qi, Xiaogang Wang, and Jiaya Jia. Pyramid scene parsing network. In *Proceedings of the IEEE conference on computer vision and pattern recognition*, pages 2881–2890, 2017.
- [96] Yuan Zhao, Bo Liu, Ming Ding, Baoping Liu, Tianqing Zhu, and Xin Yu. Proactive deepfake defence via identity watermarking. In *Proceedings of the IEEE/CVF Winter Conference on Applications of Computer Vision*, pages 4602–4611, 2023. [2](#)
- [97] Peng Zhou, Xintong Han, Vlad I Morariu, and Larry S Davis. Learning rich features for image manipulation detection. In *Proceedings of the IEEE conference on computer vision and pattern recognition*, pages 1053–1061, 2018. [2](#), [5](#)
- [98] Tian Zhou, Ziqing Ma, Qingsong Wen, Xue Wang, Liang Sun, and Rong Jin. Fedformer: Frequency enhanced decomposed transformer for long-term series forecasting. In *International Conference on Machine Learning*, pages 27268–27286. PMLR, 2022. [4](#)
- [99] Xinshan Zhu, Yongjun Qian, Xianfeng Zhao, Biao Sun, and Ya Sun. A deep learning approach to patch-based image inpainting forensics. *Signal Processing: Image Communication*, 67:90–99, 2018. [2](#)
- [100] Peiyu Zhuang, Haodong Li, Shunquan Tan, Bin Li, and Jiwu Huang. Image tampering localization using a dense fully convolutional network. *IEEE Transactions on Information Forensics and Security*, 16:2986–2999, 2021.